Lawrence Berkeley National Laboratory

Title
HYDROGEN EMBRITTLEMENT STUDIES OF A TRIP STEEL

Permalink
https://escholarship.org/uc/item/32s5c1qk

Author
Mccoy, R.A.

Publication Date
1972-07-01

LBL-439
Preprint

RECEIVED
LAWRENCE
RADIATION LABORATORY

DOCUMENTS SECTION

HYDROGEN EMBRITTLEMENT STUDIES OF A TRIP STEEL

R. A. McCoy and W. W. Gerberich

July 1972

LBL-439

DISCLAIMER

HYDROGEN EMBRITTLEMENT STUDIES OF A TRIP STEEL

R. A. McCoy and W. W. Gerberich

Inorganic Materials Research Division, Lawrence Berkeley Laboratory and
Department of Materials Science and Engineering, College of Engineering;
University of California, Berkeley, California

ABSTRACT

The conditions of cathodic charging, gaseous hydrogen environment,
and loading for which a TRIP steel may or may not be susceptible to
hydrogen embrittlement were investigated. In the austenitic state,
the TRIP steel appeared to be relatively immune to hydrogen embrittlement.
It was shown that it is the strain-induced martensitic phase, α', which
is embrittled. In TRIP steel single-edge-notch specimens under fixed
loads in gaseous hydrogen, slow crack growth occurs when the stress
intensity level exceeds a threshold level of about 25 ksi-in.$^{1/2}$
and the growth rate varies approximately as the 2.5 power of the stress
intensity level. The activation energy for this slow crack growth was
found to be about 10,000 cal/g-atom, the approximate activation for
hydrogen diffusion in martensite. Thus it was concluded that slow
crack growth in TRIP steel loaded in gaseous hydrogen involves the
diffusion of hydrogen through the α' phase.

I. INTRODUCTION

High-strength ferritic and martensitic steels are notoriously susceptible to hydrogen-induced failure—commonly called hydrogen embrittlement (H. E.). Hydrogen can be acquired by these steels relatively easily during steelmaking or processing, or from their environment while in service.[1,2,3] The mechanism by which hydrogen embrittles ferrite and martensite is still in dispute. Also, it is not well understood why austenite is relatively immune to H. E. Because of the widespread commercial use of high-strength steels and because insufficient knowledge of the influence of composition, processing, design, and environment continues to contribute to service failures, further study in the area of H. E. is of special technological importance.

A new class of potentially useful high-strength steels, TRIP steels (TRansformation Induced Plasticity), obtain their high elongation[4] and fracture toughness[5] from the strain-induced austenite to martensite transformation. In 1969 Dulis and Chandhok[6] reported that cathodically charged TRIP steel specimens were immune to hydrogen cracking. However during that same year, Gold and Koppenaal[7] reported that TRIP steels could be embrittled under certain conditions of temperature and strain rate. At the outset of this study it was hypothesized that in the austenitic state, TRIP steels should be relatively immune to H. E.; whereas, after the strain-induced transformation begins, adverse effects might be expected.

Accordingly in this investigation, the following objective was sought: The determination and understanding of the conditions of cathodic charging, gaseous hydrogen environment, and loading for which TRIP steels

may or may not be susceptible to H. E. Pursuant to this objective, appropriate experiments were designed and performed using tensile and single-edge-notch (SEN) specimens which had been cathodically charged with hydrogen or mechanically tested in pure H_2.

II. EXPERIMENTAL

A. Material Selection and Preparation

The compositions and processing of the steels tested in this investigation are listed in Table I. The thermomechanical treatment chosen for alloy C was considered to be optimal for this particular TRIP Steel.[8] As a check on the H. E. test procedures and for a comparison of H. E. properties with TRIP steel, alloy 4340, which is a tempered martensitic steel with yield and ultimate tensile strengths approximately equal to alloy C, was also evaluated.

Tensile and SEN specimens were machined from rolled sheets of these alloys. Each tensile specimen contained a gage section 1 in. long, 1/8 in. wide, and 1/10 in. thick. The SEN specimen was 2 in. × 1 in. × 1/10 in. with a side notch 0.27 in. long. The pin holes were located 1/6 in. from the centerline on the notch side, resulting in approximately crack line loading. All specimens were longitudinal, i.e., the long direction of the specimen was parallel to the rolling direction of the material. Prior to hydrogen charging or testing each SEN specimen, a fatigue crack about 0.06 in. long was produced at the root of the notch by cycling the load on a tension-tension fatigue machine between stress intensity levels of 5 to 30 ksi-in.$^{1/2}$ for about 10,000 cycles.

B. Fracture Mechanics for the SEN Specimen

For the SEN specimen, the relationship between the stress intensity factor K, the applied load P, and the specimen dimensions has been established by compliance experiments[9] and by mathematical stress analysis procedures.[10] This expression is:

$$K = \frac{YP}{(1 - \nu^2)^{1/2} \, BW^{1/2}} \qquad\qquad (1)$$

where Y = a dimensionless factor which is a function of a/W

a = crack length

ν = Poisson's ratio

B = specimen thickness

W = specimen width

If the load is increased until the crack begins to grow, i.e. becomes unstable, the critical load P_c and critical crack length a_c determine a critical stress intensity factor K_{cr} from Eq. (1). Under dead-weight loading, the specimen would fail catastrophically upon reaching K_{cr}. At this critical point in the Instron testing machine, however, the load simply decreases as the crack grows. For any crack length such that $a < \frac{W}{2}$, the critical load for further crack growth will yield the same value of K_{cr} as derived from Eq. (1). Thus, K_{cr} can be used as a relative measure of fracture toughness of a material. As the thickness of a fracture specimen increases, the value of K_{cr} approaches the lower limiting value, the plane-strain fracture toughness K_{Ic}. Because the material near the surface is nearly in a plane-stress condition whereas the midthickness material is approximated by a plane-strain condition, the measured K_{cr} will be somewhat higher than the true K_{Ic}. However, because the dimensions of all the SEN specimens tested in this investigation were nearly the same, comparison of their K_{cr} values relative to each other appears justified.

C. Hydrogen Charging Procedures

Although the term H. E. has most often referred to embrittlement of steels containing "internal" or absorbed hydrogen introduced, for example, during cathodic charging, it may also refer to embrittlement of previously hydrogen-free steels which have been strained or loaded in gaseous hydrogen environments. Accordingly, to study H. E. of TRIP steels by both modes of hydrogen introduction, the following two techniques were employed in this investigation:

1. Cathodic charging in an acid electrolyte.

The entry of electrolytic hydrogen from an acid solution into a steel specimen acting as a cathode can be expressed as[11]

$$H^+ + Fe + e^- \longrightarrow Fe\text{-}H_{ads} \begin{cases} 1/2\ H_2 \uparrow\ +\ Fe \\ Fe\text{-}H_{abs} \end{cases} \qquad (2)$$
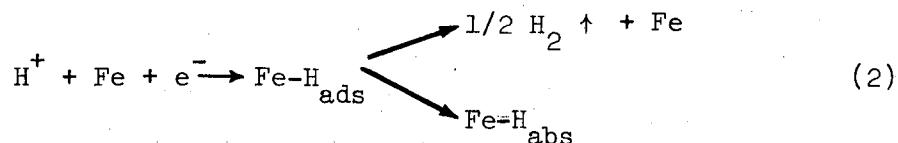
where $Fe\text{-}H_{ads}$ refers to adsorbed hydrogen on the metal surface and $Fe\text{-}H_{abs}$ refers to absorbed hydrogen directly beneath the metal surface. The absorbed hydrogen atoms or ions occupy interstitial positions in the lattice.[12] Under the driving force of concentration and/or stress gradients, the hydrogen may diffuse to various locations within the metal.[13]

The electrolytic cell used to perform all the cathodic charging of specimens in this investigation consisted of a specimen to be charged as the cathode, a platinum anode, and a thermometer all immersed in an electrolyte. The charging temperature was maintained at the arbitrary value of 38°C. The electrolyte was dilute sulfuric acid with or without

the addition of a poison, either arsenic or white phosphorus.* The

poison addition, the concentration of the acid, the current density and

the charging time were left as charging variables.

Because the diffusivity of hydrogen is about four orders of mag-

nitude less in fcc than in bcc steel,[12] cathodic charging is a poor

technique to introduce hydrogen into the austenitic TRIP steels. As will

be discussed later, there was evidence that cathodic charging of TRIP

steel resulted in a sharp hydrogen concentration gradient with a high

concentration at the surface. Moreover, hydrogen analysis using a hot

vacuum extraction method failed to indicate any significant increase

in the average hydrogen content in TRIP steel due to cathodic charging.

Because of these reasons, the major thrust of the investigation was

turned away from cathodic charging and directed at testing the specimens

in a pure hydrogen atmosphere.

2. Mechanical testing in H_2.

Only in the last few years have studies of H. E. using a gaseous

hydrogen environment method been reported.[14-20] With this method,

gaseous hydrogen available at the crack tip is adsorbed onto the clean

surface provided at the stressed crack tip.[20] Thus, the crack tip sur-

face acts as an immediate and constant source of hydrogen which may

readily undergo short range diffusion, driven by stress gradients, to

the area of maximum triaxiality ahead of the crack tip. This manner

of investigating H. E. is not complicated by a number of poorly under-

stood phenomena which enter into electrolytic H. E. tests such as the

permeation of hydrogen as a function of cathodic charging condition,

---

*
 For the exact concentrations of the acid and poisons used, see the
results section.

composition, amount of cold work, microstructure, etc. of the steel.
Also avoided by using gaseous H. E. tests is the problem of performing
an accurate analysis for the hydrogen content.

For these gaseous H. E. tests, a special Lucite cylindrical chamber,
2 in. O.D., 4 1/2 in. long, and 1/8 in. wall, was constructed with an
inlet and an outlet for introducing pure, dry hydrogen and purging the
chamber of air. O-rings on the specimen grips sealed in gas with pressures
up to 60 psig* without leaking. Either tensile or SEN specimens could be
tested in the chamber. For testing a specimen in hydrogen at a temper-
ature other than at room temperature, a steel housing for the Lucite
chamber was constructed so that during the test the specimen-chamber-housing
assembly could be immersed in a bath of water chilled or heated to a
specific temperature.

D. Mechanical Testing

To be able to compare relative strength levels and ductilities, sev-
eral alloy specimens were tensile tested on an Instron at room temperature,
at a strain rate of 0.04 min^{-1}. These properties are shown in Table II.
Additional tensile tests were performed incorporating various combina-
tions of the following variables: a) severity of cathodic charge,
b) testing atmosphere: air or H$_2$ at various pressures, and c) strain
rate. When the yield point on the stress-strain curve was not clearly
defined, the stress corresponding to 0.2% offset in strain was reported
as the yield stress. The elongation reported throughout this investi-
gation is total elongation within the 1 in. gage length.

A wide variety of slow-crack-growth tests, both dynamic and static,

---

* psig means gage pressure above ambient pressure.

were performed on SEN specimens with a) severity of cathodic charge, b) testing atmosphere: air or 15 psig H_2, c) strain rates, d) stress intensity level, and e) temperature being the variables.

III. RESULTS

A. Cathodically Charged SEN Specimens
Tested at Fixed Loads

This phase of the investigation has been reported in detail in an earlier publication.[21] In these reported tests as well as in several more recent tests, TRIP steel SEN specimens were given cathodic charges several orders of magnitude more severe than conventional cathodic charges.[2,20] Subsequent to cathodic charging and cadmium plating, each specimen was held at a constant load corresponding to 80% K_{cr} for about 8 hours. In 13 tests on TRIP steel specimens, there were no instances of hydrogen-induced, delayed, brittle failures nor appreciable slow crack growth.

Metallographic examination of the H. E. tested SEN specimens did, however, reveal a crack network near the specimen surface and within the plastic zone, shown in Fig. 2 of McCoy, et al.[21] This C-shaped network extended about 0.05 in. ahead of the fatigue crack. After etching, it was evident that the cracks followed along paths of martensite plates formed during loading. This observation supports one of the initial hypotheses of this investigation that while the α' martensite can be hydrogen embrittled, the surrounding austenite cannot. Near the midthickness of the specimens, the amount of cracking occurring in the hydrogen-bearing martensite was far less than at the surface. This smaller amount of cracking at the center may be due to a smaller amount of martensite and/or to a lower level of hydrogen concentration.

B. Cathodically Charged SEN Specimens Tested Under Dynamic Loading

Charged and uncharged SEN specimens of alloy C were tested in the Instron at various crosshead speeds, as shown in Table III. If H. E. were occurring during the test, subcritical slow crack growth would be expected. Hence at slow crosshead speeds, the crack would grow and lower the apparent K_{cr} which was calculated using the maximum load for P_c and the initial crack length for a_c in Eq. (1). This initial crack length was measured at the midthickness after fracture and included a plastic zone of 0.04 in. However, the results showed no appreciable drop in K_{cr} for the charged specimens, indicating that no slow crack growth due to an embrittling process had occurred.

C. Cathodically Charged Tensile Specimens

Tensile specimens of alloy C and of 4340 were charged in electrolyte B (2 normal H_2SO_4 with 3 ppm arsenic) at 1.2 amp/in.^{2} for one hour and subsequently tensile tested at room temperature. The resulting tensile properties are shown in Table IV. Figure 1 shows that the embrittlement in the cathodically charged TRIP steel tensile specimens is evidenced as premature failure which curtails the elongation usually gained by the TRIP spenomenon. The basic ductility of the steel as measured by the R. A., however, remains nearly constant at about 60% of the R. A. of the uncharged specimens as the charging time increases. Figure 1 suggests that by increasing charging times and hence with a greater amount of diffusive hydrogen available, less time is required to build up to the critical hydrogen concentration needed for the embrittlement process.

The cathodically charged 4340 specimen failed while in the elastic

region at a stress level about one quarter of the yield strength. This fact added to the negligible elongation and 5% reduction of area demonstrates clearly the effectiveness and severity of the cathodic charging procedure.

To determine whether the cathodic charging procedure produces any permanent structural damage to the specimen, two specimens of alloy C were charged in electrolyte B for 6 1/2 hours at 1.2 amp/in.^{2}. Before testing, one specimen was baked 16 hours at 200°C. Then both specimens were tensile tested at a strain rate of 0.002 min^{-1}. The unbaked specimen was embrittled after an elongation of 2.5% and R. A. of 20%. Notably different, however, was the baked specimen with the ductility expected of an uncharged specimen: elongation of 42% and R. A. of 38%. Apparently the baking process removed all of the damaging hydrogen. Demonstrated also was that the H. E. was reversible and the charging procedure caused to permanent structural damage to the specimen.

D. Tensile Specimens Tested in H_2

Tensile specimens of alloy C were tested in air and in 30 psig H_2 at various strain rates and the resulting ductility and temperature rise due to adiabatic heating are shown in Fig. 2. When tested at slow strain rates in H_2, the loss of ductility was quite severe--a loss of elongation of 94% and a loss of R. A. of 57% relative to the same test run in air.

E. SEN Specimens Tested in H_2 Under Dynamic Loading

The conditions and results of testing SEN specimens of alloy C in hydrogen at several strain rates are shown in Table III. While at the fast crosshead speed, there was no drop in the K_{cr}. At slower crosshead

speeds, however, there was a significant drop in the K_{cr} indicating

that slow crack growth had occurred. An approximate value for the slow

crack growth Δa was measured using a traversing microscope during the

test. Calculating K'_{cr} based upon the initial crack length plus Δa resulted

in values close to the K_{cr} of the other specimens which deomonstrated no

slow crack growth. Thus it appears that the critical stress intensity

factor for unstable rapid crack growth is a basic property of the material

and remains unchanged, whether preceded by slow crack growth or not.

F. SEN Specimens Tested in H_2 at Fixed Loads

Slow crack growth rates of SEN specimens of alloy C in 15 psig H_2

were measured with the traversing microscope at numerous stress intensity

levels and at three different temperatures. These results are plotted

in Fig. 3. Although the curves for the three temperatures appear to be

nearly parallel, the slopes increase slightly as the temperature increases.

At room temperature, the slopes correspond to a relationship of

$$\frac{da}{dt} \alpha K^{2.5}$$

If the thermally activated process is assumed to be of the Arrhenius

type, i.e.

$$\frac{da}{dt} = Ae^{-Q/RT}$$

then the activation energy Q can be computed from the slope of the curve

for $\log \frac{da}{dt}$ versus $1/T$ at a specific stress intensity level. At $K = 50$

ski-in.$^{1/2}$, an activation energy of $10,100 \pm 250$ cal/g-atom was obtained,

as shown in Fig. 4. At higher stress intensity levels, higher values

of Q were found because at the higher crack growth rates adiabatic

heating in the plastic zone possibly results in a shift in the embrittling mechanism. Although Q may have a slightly lower value for K below 50 ksi-in.$^{1/2}$, the value of Q = 10,100 cal/g-atom will be considered most representative of the activation energy of the slow crack growth of alloy C around room temperature.

The slow crack growth of one of the alloy C specimens in H_2 was monitored with stress wave emission (SWE) equipment. From the stress wave emitted each time the crack advances, it is determined that the crack growth was discontinuous, separated by short secondary incubation periods. This discontinuous nature of slow crack growth has also been found in high-strength martensitic steels that were cathodically charged or tested in distilled water.[22,23]

IV. DISCUSSION

A. Cathodically Charged Versus Gaseous Hydrogen Embrittlement

A TRIP steel specimen tensile tested in 15 psig H_2 (see Table IV) has approximately the same loss of ductility as a specimen cathodically charged about 45 minutes in electrolyte B. Tests on the alloy 4340, however, show that with a tempered martensitic steel, the H_2 environment results in much less loss of ductility than the cathodic charge, as shown in Table IV. Remember that this cathodic charge is several orders of magnitude more severe than that used in conventional H. E. tests on tempered martensitic steels.[2,20]

A plausible explanation of the observed differences in behavior between tensile specimens of TRIP steel and tempered martensite is based upon the fact that the hydrogen diffusivity in fcc is about four orders of magnitude slower than that in bcc. During cathodic charging of the austenitic TRIP steel, only the surface layer builds upon hydrogen. Hence, when α' starts to form during the tensile test, only the α' in the surface layer becomes embrittled. This embrittlement is first evidenced by microcracks forming at the embrittled α' plates followed by the coalescence of these microcracks into a macrocrack, thus resulting in slow crack growth from the surface inward. If the α' below the surface contains an insufficient hydrogen concentration, the cracking will stop, leaving cracks only in the surface layer. In TRIP steel tensile specimens if the cathodic charge is severe enough, slow crack growth will progress far enough as to appreciably reduce the effective load carrying cross sectional area. This causes a higher stress on the remaining material resulting in a premature but ductile failure which precludes much of the usual elongation derived from the TRIP process.

On the other hand, for the tempered martensitic steel in which hydrogen diffusion is relatively rapid, the cathodic charging procedure easily and quickly supplies hydrogen throughout the specimen. A 4340 steel charged 5 minutes in 4% H_2SO_4 with a phosphorus poison at 0.01 amp/in.^{2} (two orders of magnitude less than that used in this investigation) results in considerable embrittlement.[2] Thus, the severe embrittlement resulting from a 60 minute charge in electrolyte B (9.4% H_2SO_4) at 1.2 amp/in.^{2} of the 4340 specimen shown in Table IV is not surprising.

Specimens tested in H_2 adsorb hydrogen onto their surfaces followed by at least some degree of short range diffusion inward. Oriani[13] suggests that the adsorption of hydrogen upon a clean metal surface results in a full monolayer of atomic hydrogen on the surface and that the concentration of hydrogen drops off sharply in distance inward from the surface. If the time involved, hydrogen diffusivity, and driving force (concentration and/or stress gradients) are greater enough, long range diffusion may be considerable. But because of the relatively low hydrogen diffusivity in austenite, it is quite probable that for TRIP steel specimens in H_2 only the material very near the surface would contain relatively high concentrations of hydrogen. As with the cathodically charged specimen when the α' begins to form during the tensile test, only the α' near the surface is embrittled. Thus, one would expect and indeed finds that the resulting properties of this specimen are similar to those of a specimen that had been cathodically charged. Comparison of the fracture surfaces of TRIP steel tensile specimens representing both modes of hydrogen entry verifies that in each case slow crack growth originated at the surface.

For TRIP steel SEN specimens tested in H_2, the surface layer at the crack tip always contains a relatively high concentration of hydrogen. With the application of a tensile load on the SEN specimen, a plastic zone containing α' is formed ahead of the crack tip. Since this particular TRIP steel is relatively unstable at room temperature, the volume fraction of martensite near the crack tip approaches unity.[24] Therefore, the strain-induced martensite at the crack tip is quite likely to form a continuous network as it appears in Fig. 1 of Ref. 21. Hydrogen in the crack tip surface layer diffuses under the driving force of a stress gradient through the α' to the region with the highest triaxial stress state[13,25] (hydrostatic tension) located a short distance ahead of the crack tip. Microcracks along the α' plates form in this region. As the material between the microcracks fractures, the microcracks coalesce and connect up with the main crack. Slow crack growth, therefore, consists of discontinuous jumps as the microcracks join the advancing main crack. The time between each jump is the observed secondary incubation time.

Figure 5 consists of scanning electron microscope (SEM) fractographs of SEN specimens loaded in 15 psig H_2. The fracture surface regions of slow crack growth as shown in Fig. 5 appear very similar to regions of slow crack growth in TRIP steel tensile specimens that were cathodically charged or that were tested in H_2.

A tentative explanation is now offered as to why the cathodically charged TRIP steel SEN specimens failed to exhibit significant slow crack growth as was exhibited by the SEN specimens tested in H_2.

Following a cathodic charge, only the surface layer and the area ahead of the crack tip contain a relatively high concentration of hydrogen. The area ahead of the crack tip contains a higher hydrogen concentration because of a small amount of martensite formed in this region during fatigue precracking prior to charging.[21] When a charged SEN specimen is loaded in tension, the α' formed in the surface layer and ahead of the crack tip is embrittled which results in surface cracks and a slight extension of the main crack. Unlike a specimen tested in H_2 which has an abundant supply of hydrogen always available at the crack tip, a charged specimen has a very limited hydrogen supply. Besides the fact that the crack grows out of the region of higher hydrogen content after some initial cracking, the stress gradient in the material near the cracked α' plates at the crack tip is greatly reduced. Hence, the hydrogen contained in this material has a much smaller driving force for diffusion inward ahead of the crack tip. Because of these effects, not enough hydrogen can build up in the region of maximum triaxiality to result in the further embrittlement of the α' and further slow crack growth is impossible.

B. Comparison of a Phenomenological Expression for Crack Growth Rate with Experimental Results

Gerberich, et al.[22,23,26] investigated the crack growth process in SEN specimens of a high-strength tempered martensitic steel tested in the cathodically charged condition, in distilled water, and in combination. From SWE analysis coupled with fracture mechanics they developed a model for the crack growth process consisting of discontinuous steps, each with an average jump size of

$$\ell^* \approx \frac{2\nu_c}{\pi\varepsilon_f} \approx \frac{(K - K_{scg})^2}{2\pi\,\sigma_{ys}\,E\varepsilon_f} \qquad (3)$$

where

$2\nu_c$ = theoretical crack tip displacement

ε_f = fracture strain

K_{scg} = threshold stress intensity factor for slow crack growth

σ_{ys} = tensile yield stress

E = modulus of elasticity

Also the time between stress waves or crack jumps, the secondary incubation time, Δt_s, was found to remain nearly constant. Assuming the diffusion of hydrogen from one crack site to the next is the controlling mechanism,[27] then

$$\Delta t_s \approx \frac{C\,d^2}{D} \qquad (4)$$

where

d = cleavage facet size

D = hydrogen diffusivity = $D_o e^{-Q/RT}$

C = a constant

Thus the crack growth rate can be approximated by

$$\frac{da}{dt} = \frac{\ell^*}{\Delta t_s} = \frac{(K - K_{scg})^2\,D}{2\pi\,\sigma_{ys}\,E\,\varepsilon_f\,C\,d^2} \qquad (5)$$

To test this crack growth rate equation against the experimental results obtained for TRIP steel SEN specimens tested in H_2 in this investigation as shown in Fig. 3, the following values were used in Eq. (5).

$K_{scg} \approx 25$ ksi-in.$^{1/2}$

$\sigma_{ys} = 220$ ksi (from Table II)

$E = 30 \quad 10^6$ psi

$\varepsilon_f \approx 0.1$

$D = 3.2 \times 10^{-7}$ cm^2/sec (for martensitic steel at room temperature

from Hobson[28])

$Cd^2 \approx 25 \times 10^{-8}$ in.^{2}

Prior to calculation, it is appropriate to discuss the bases of these choices. First, consider the threshold stress intensity, K_{scg}. Under limited-time conditions of the present investigation, no slow crack growth was observed for stress intensity levels below 40 ksi-in.$^{1/2}$. On the other hand, a similar TRIP steel[26] was found to have a threshold stress intensity of about 10 ksi-in.$^{1/2}$ under fatigue conditions. There-fore, an estimate of 25 ksi-in.$^{1/2}$ for static loading conditions would be a reasonable first approximation.

Considering the fracture ductility, the value for the TRIP steel in Table IV is seen to be similar to the 4340 steel when tested in H_2. The appropriate value is the true fracture strain at the tip of the crack. Depending on the degree of plane strain conditions, this value can be about 1/3 to 1/2 of the tensile situation, or in the case of the 15 psig test, would range from 0.095 to 0.14. That is,

$$\varepsilon_{f_{(crack)}} \approx \frac{1}{3} \varepsilon_{f_{(tensile)}} \approx \frac{1}{3} \ln \frac{1}{1 - R.A.} \approx 0.10 \qquad (6)$$

With respect to hydrogen diffusivity, the value of D as taken from observations in a totally martensitic structure might be high for an austenite-martensite mixture unless the strain-induced martensite

represents a relatively continuous path for hydrogen diffusion at the tip of a crack. As mentioned earlier the volume fraction of martensite close to the crack tip approaches unity. Since the hydrogen source would be at and/or behind the crack tip where the martensite content would be large, the present assumption of D is not too unrealistic. Of course, for substantially more stable metastable austenites, this analysis would require modification.

Finally, an exact value of Cd^2 is not possible to ascertain. Nevertheless, an estimate can be made based upon the size of fracture nucleation sites noted in Fig. 5D, which on the average are about 4μ or 1.57×10^{-4} in. Since the value of the constant, C, corresponding to the cathodically charged case can range from two to twenty,[26] a value of 10 is used here giving $Cd^2 \approx 25 \times 10^{-8}$ in.$^{-2}$.

These values in conjunction with Eq. (5) give:

K(ksi-in.$^{1/2}$)	$\frac{da}{dt}$ (mils/min)
60	3.5
80	8.6
100	16.1

These points plotted as * in Fig. 3 are seen to lie near the experimental curve at room temperature. Although the data are about a factor of two low compared to the observations, slightly different but plausible choices for D, ε_f and Cd^2 could easily account for this relatively small deviation. The fact that a model derived for cathodically charged steel gave a reasonable correlation to data obtained from gaseous hydrogen embrittlement was either very fortuitous or indicative that

both gaseous hydrogen and cathodically charged H. E. mechanisms are based

upon the bulk diffusion of hydrogen.

<div align="center">

C. Comparison of Experimental Results
with Other Published Results

</div>

This investigation found an activation energy of 10,100 cal/g-atom

for the slow crack growth in TRIP steel tested in 15 psig H_2 around

room temperature. This value falls very close to the 9500 to 9800 cal/

g-atom range found by other investigators[25,29-32] as characteristic of

either hydrogen diffusion or the measurable quantities related to H. E.

in high-strength martensitic steels, listed in Table I of Johnson.[20]

Moreover, from measurements of the embrittling temperature for TRIP

steel tensile specimens tested at various strain rates, Gold and Koppenaal[7]

determined at activation energy of 9900 cal/g-atom. Also Birat[33] has

recently reported an activation energy of 10,200 cal/g-atom for the crack

growth rate for TRIP steel SEN specimens fatigued in distilled water.

The activation energy for hydrogen diffusion in fcc steel has been

reported to be around 13,000 cal/g-atom.[12] Thus, it is concluded that

the slow crack growth in gaseous hydrogen involves the diffusion of

hydrogen through the α' phase of the TRIP steel.

Williams and Nelson[19] investigated the embrittlement of 4130 steel

by low-pressure gaseous hydrogen. They explain their results by means

of an adsorption mechanism for the slow crack growth in which hydrogen

adsorption is the rate controlling step. Moreover, they state, ". . . no

bulk hydrogen diffusion is required for gaseous hydrogen embrittlement.

Therefore, no 'incubation time' should be required for gaseous hydrogen

embrittlement." However, Gerberich and Hartbower[23] found from SWE

studies of cathodically charged martensitic steel specimens which had
been fatigue precracked that a) slow crack growth was discontinuous and
b) secondary incubation times during slow crack growth were not appreciably
different from the primary incubation time (prior to slow crack growth).
As described earlier, the SWE study in this investigation on a TRIP steel
SEN specimen tested in H_2 revealed that the slow crack growth was dis-
continuous and exhibited secondary incubation times.

   These results added with the activation energy obtained in this
study suggest that a bulk transport mechanism might be controlling in
the case of gaseous hydrogen embrittlement, at least in metastable
austenitic steels.

V. CONCLUSIONS AND SUMMARY

The conclusions regarding the H. E. characteristics of TRIP steels based upon the experiments in this investigation are:

1. In the austenitic state, TRIP steels are relatively immune to H. E. It is the α' phase which is embrittled.

2. Subsequent to yielding in tensile tests, the embrittled α' leads to premature failures which exhibit less elongation as either the severity of the cathodic charge or the H_2 pressure is increased and as the strain rate is decreased.

3. In TRIP steel SEN specimens under fixed loads in H_2, slow crack growth occurs when the stress intensity level exceeds a threshold level K_{scg} of about 25 ksi-in.$^{1/2}$ and the growth rate varies approximately as the 2.5 power of K.

4. The activation energy for this slow crack growth is about 10,000 cal/g-atom, the approximate activation energy for hydrogen diffusion in α'.

Finally, the present investigation strongly indicates that a H. E. mechanism based upon bulk hydrogen diffusion in the α' phase best explains the present data, at least in the case of metastable austenitic steels.

REFERENCES

1. P. Cotterill, Progress in Materials Science, B. V. Chalmers, ed., (Pergamon Press, New York, 1961) vol. 9, pp. 205-301.

2. A. R. Elsea and E. E. Fletcher, Hydrogen-Induced, Delayed, Brittle Failures of High-Strength Steels, DMIC Report 196, Battelle Mem. Inst., January 1964.

3. M. Smialowski, Hydrogen in Steel (Pergamon Press, New York, 1962).

4. V. F. Zackay, E. R. Parker, D. Fahr and R. Busch, ASM Trans. Quart 60, 252 (1967).

5. W. W. Gerberich, P. L. Hemmings, V. F. Zackay and E. R. Parker, Fracture 1969, P. L. Pratt, ed., (Chapman and Hall, Ltd., London, 1969) pp. 288-305.

6. E. J. Dulis and V. K. Chandohk, Metals Progress 97, 101 (1969).

7. E. Gold and T. J. Koppenaal, ASM Trans. Quart 62, 607 (1969).

8. D. Fahr, Enhancement of Ductility in High Strength Steels (Ph. D. Thesis), UCRL-19060, September 1969.

9. A. M. Sullivan, Materials Res. Stds. 4, 20 (1964).

10. B. Gross and J. E. Srawley, Stress Intensity Factors for Single-Edge-Notch Specimens in Bending or Combined Bending and Tension by Boundary Collocation of a Stress Function, NASA TN D-2603, 1965.

11. J. McBreen and M. A. Grenshaw, Fundamental Aspects of Stress Corrosion Cracking, R. A. Staehle, A. J. Forty and D. van Rooyen, eds., National Association of Corrosion Engineers, Houston, 1969, pp. 51-63.

12. E. E. Fletcher and A. R. Elsea, DMIC Report 219, Battelle Mem. Inst., June 1965.

13.   R. A. Oriani, Hydrogen in Metals, ibid, Ref. 11, pp. 32-50.

14.   A. S. Tetelman, The Mechanism of Hydrogen Embrittlement in Steel,
      ibid, Ref. 11, pp. 446-464.

15.   G. G. Hancock and H. H. Johnson, Trans. TMS-AIME 236, 513 (1966).

16.   R. B. Benson, Jr., R. K. Dann, and L. W. Roberts, Jr., Trans. TMS-
      AIME 242, 2199 (1968).

17.   R. M. Vennett and G. S. Ansell, ASM Trans. Quart 62, 1007 (1969).

18.   R. J. Walter, R. P. Jewett and W. T. Chandler, Mater. Sci. Eng. 5,
      98 (1969-70).

19.   D. P. Williams and H. G. Nelson, Met. Trans. 1, 63 (1970).

20.   H. H. Johnson, On Hydrogen Brittleness in High Strength Steels, ibid,
      Ref. 11, pp. 439-445.

21.   R. A. McCoy, W. W. Gerberich and V. F. Zackay, Met. Trans. 1, 2031
      (1970).

22.   C. E. Hartbower, W. W. Gerberich and P. P. Crimmins, Mechanisms of
      Slow Crack Growth in High-Strength Steels, AFML-TR-67-26, vol. 1,
      Aerojet-General Corp., Sacramento, California, February 1967.

23.   W. W. Gerberich and C. E. Hartbower, Monitoring Crack Growth of
      Hydrogen Embrittlement and Stress Corrosion Cracking by Acoustic
      Emission, ibid, Ref. 11, pp. 420-438.

24.   W. W. Gerberich, P. L. Hemmings and V. J. Zackay, Trans. TMS-AIME 245,
      1126 (1969).

25.   E. A. Steigerwald, F. W. Schaller and W. R. Troiano, Trans. TMS-AIME
      215, 1048 (1959).

26. W. W. Gerberich, J. P. Birat and V. F. Zackay, A Superposition

Model for Environmental-Assisted Fatigue-Crack Propagation, Lawrence

Berkeley Lab., Berkeley, Calif., March 1971.

27. F. J. Bradshaw and C. Wheller, Appl. Mat. Res. 5, 112 (1966).

28. J. D. Hobson, J. Iron Steel Inst. 189, 315 (1958).

29. C. F. Barth and E. A. Steigerwald, Met. Trans. 1, 3451 (1970).

30. H. H. Johnson and A. M. Willner, Appl. Mat. Res. 4, 34 (1965).

31. W. A. Van Der Sluys, Mechanisms of Environment-Induced Subscritical

Flaw Growth in AISI 4340 Steel, presented at First National Symposium

on Fracture Mechanisms, Lehigh University, 1967.

32. K. Farrell and A. G. Quarrel, J. Iron Steel Inst. 202, 1002 (1964).

33. J. P. Birat, Stress Corrosion Cracking of a TRIP Steel (M. S. Thesis)

UCRL-20300, September 1970.

34. D. Bhandarkar, Mechanical Properties of Some Metastable Austenitic

Alloys (M. S. Thesis), UCRL-19626, May 1970.

Table I. Compositions and Processing Treatments.

Alloy	Type Steel	Composition, Wt. Percent						Processing Treatment		
		C	Cr	Ni	Mo	Mn	Other	Solution Treatment (°C)	Quench Medium	Tempered or Warm Rolled (°C)
C	TRIP	0.25	8.8	8.3	3.7	2.1	2.0Si	1175 for 1 hr	Ice Brine	Rolled 80% at 425
4340	Tempered Martensite	0.40	0.8	1.8	0.25	0.7	0.3Si	1000 for 1/2 hr	Water	Tempered at 550 for 2 hr + 2 hr

Table II.   Room Temperature Tensile Properties.

Alloy	0.2% Y.S. (ksi)	U.Y.P* (ksi)	U.T.S. (ksi)	Elong. (%)	R.A. (%)
C		219	240	41	54
4340	212		248	6.3	42

*U.Y.P. is the stress at the upper yield point.

Table III. Conditions and Results of Dynamic H.E.
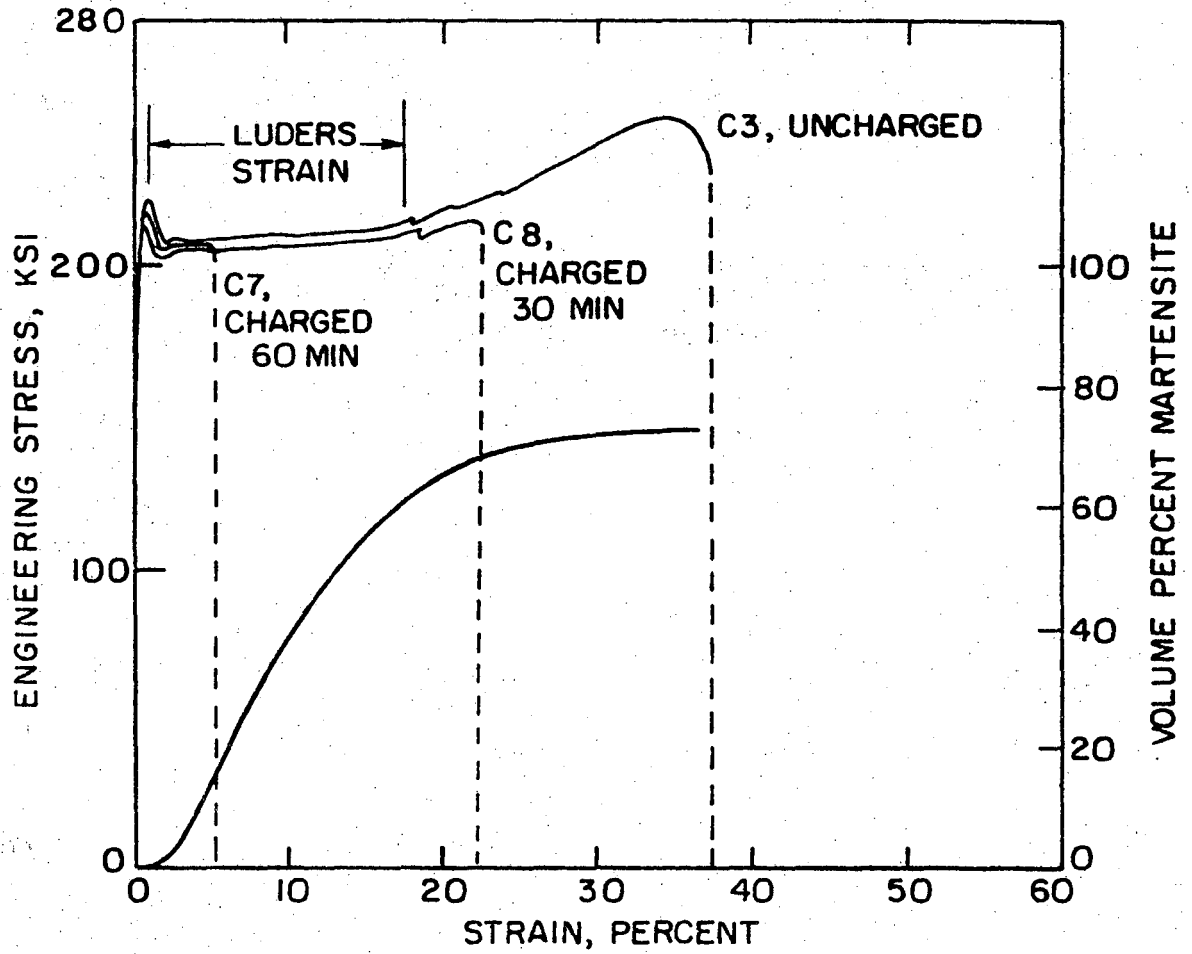Tests on SEN Specimens of Alloy C.

Type Test	Specimen	Cathodic Charge Conditions			H_2 Pressure (psig)	Cross-head Speed (in/min)	K_{cr} (ksi-in.$^{1/2}$)	Δa (mils)	K'_{cr} (ksi-in.$^{1/2}$)
		Electrolyte*	Time (min)	Current Density (amp/in.^{2})					
Air	C-11					0.20	169		
	C-3					0.04	166		
	C-4					0.04	172		
	C-17					0.004	167		
Cathodic Charge	C-1	A	50	0.125		0.04	162		
	C-2	B	50	0.125		0.04	170		
	C-19	A	60	1.2		0.002	163		
H_2	C-10				30	0.20	169		
	C-16				30	0.004	133	60	164
	C-18				15	0.002	143	55	170

*Electrolyte A consisted of one liter of 4 wt % H_2SO_4 and five drops of a poison composed of 0.5 g of white phosphorus dissolved in 10 ml of CS_2. Electrolyte B consisted of 2 normal H_2SO_4 (9.4 wt %) with 3 ppm arsenic.

Table IV. Conditions and Results of H. E. Tests on Tensile
Specimens at Strain Rate of 0.002 Min^{-1}.

| Type Test | Alloy | Cathodic Charging Conditions | | | H_2 Pressure (psig) | Room temperature tensile properties | | | | |
		Electrolyte	Time (min)	Current Density (amp/in.^{2})		0.2%Y.S. (ksi)	U.Y.P. (ksi)	U.T.S. (ksi)	Elong. (%)	R. A. (%)
Air	C						225	247	40.1	36.2
	4340					209		243	4.8	26.9
Cathodic	C	B	60	1.2			219	219	5.3	23.5
Charge	4340	B	60	1.2				56		5.3
H_2	C				15		215	215	10.5	25.0
	C				30		220	220	2.8	15.6
	4340				30	205		242	2.9	19.2

XBL719-7262

Fig. 1 Stress-strain curves for TRIP steel tensile specimens with dif-
ferent cathodic charging times in electrolyte B at 1.2 amp/in.[2].
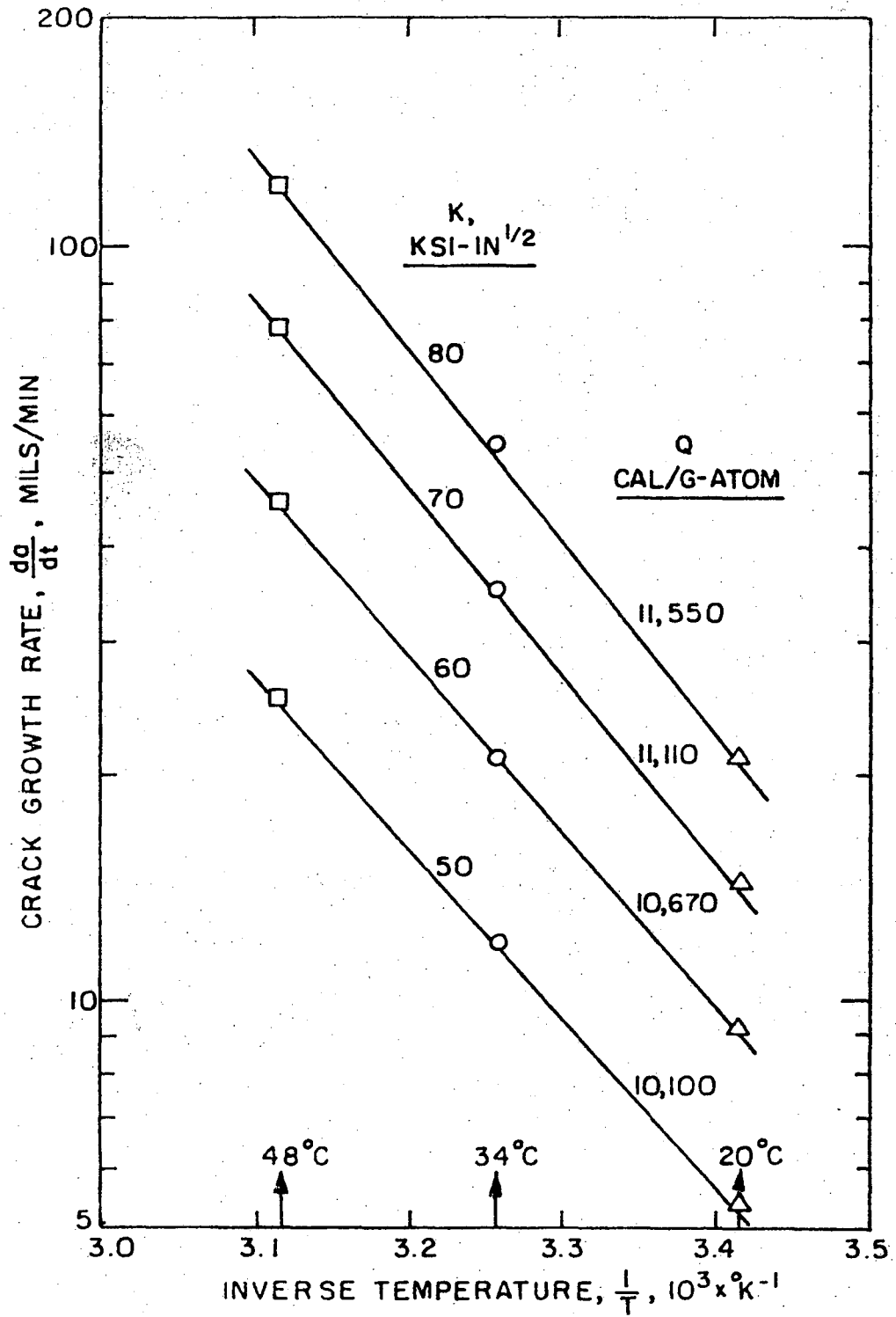Strain rate was 0.002 min^{-1}. Volume percent α' martensite data
from Bhandarkar.[34]
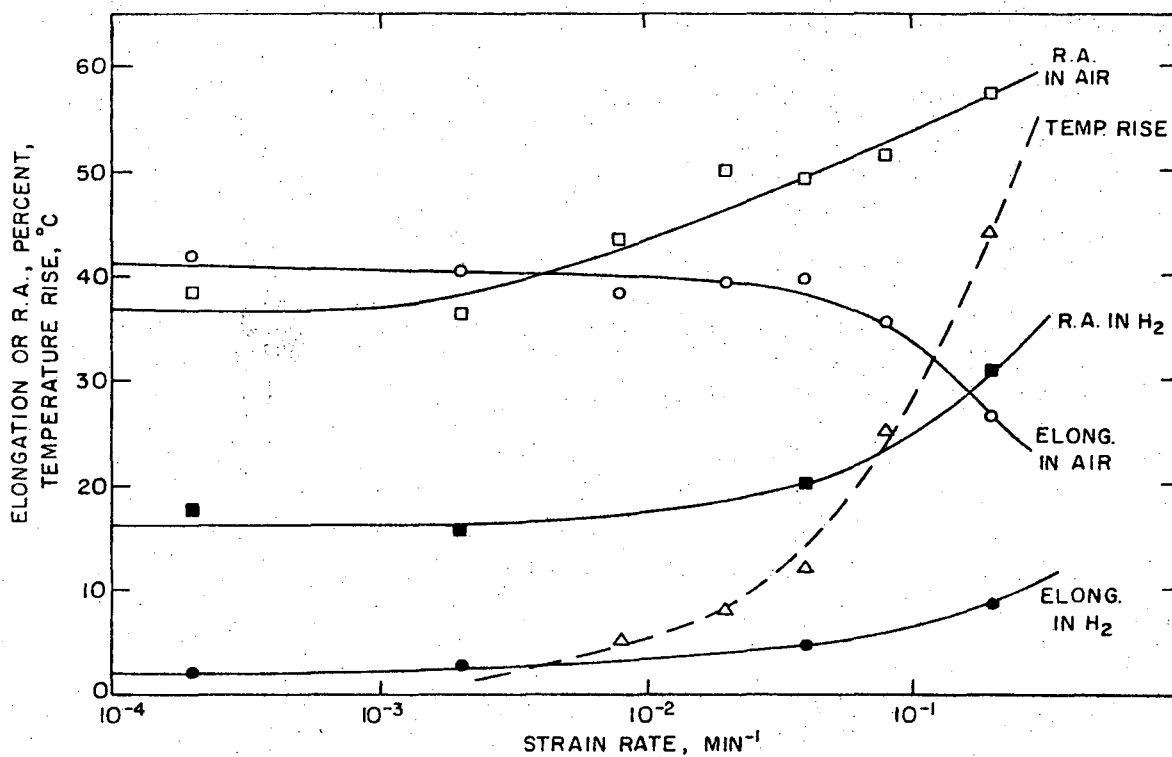
Fig. 2 Ductility and temperature rise of TRIP steel tensile specimens
tested in air or in 30 psig H_2 as a function of strain rate.
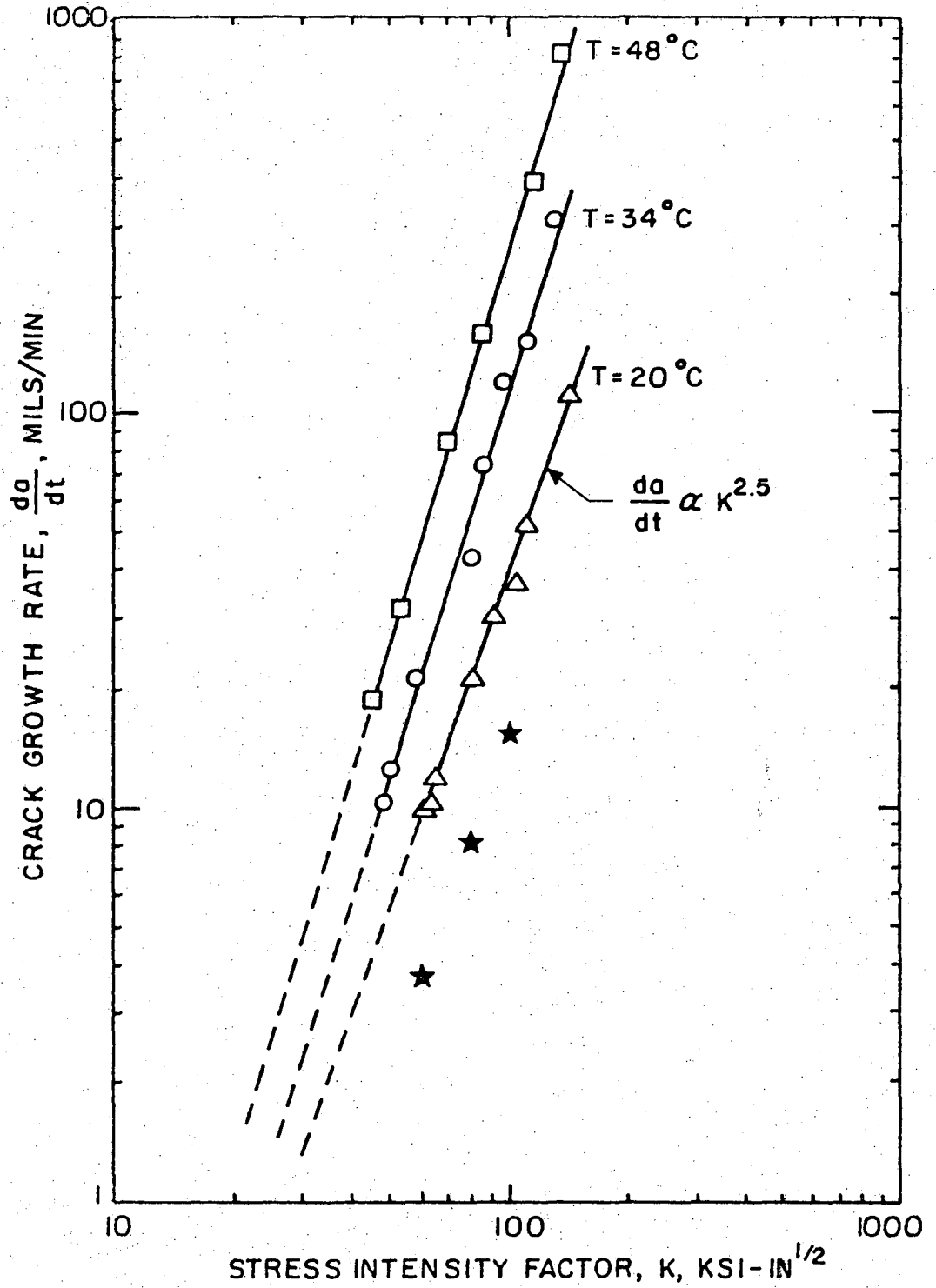
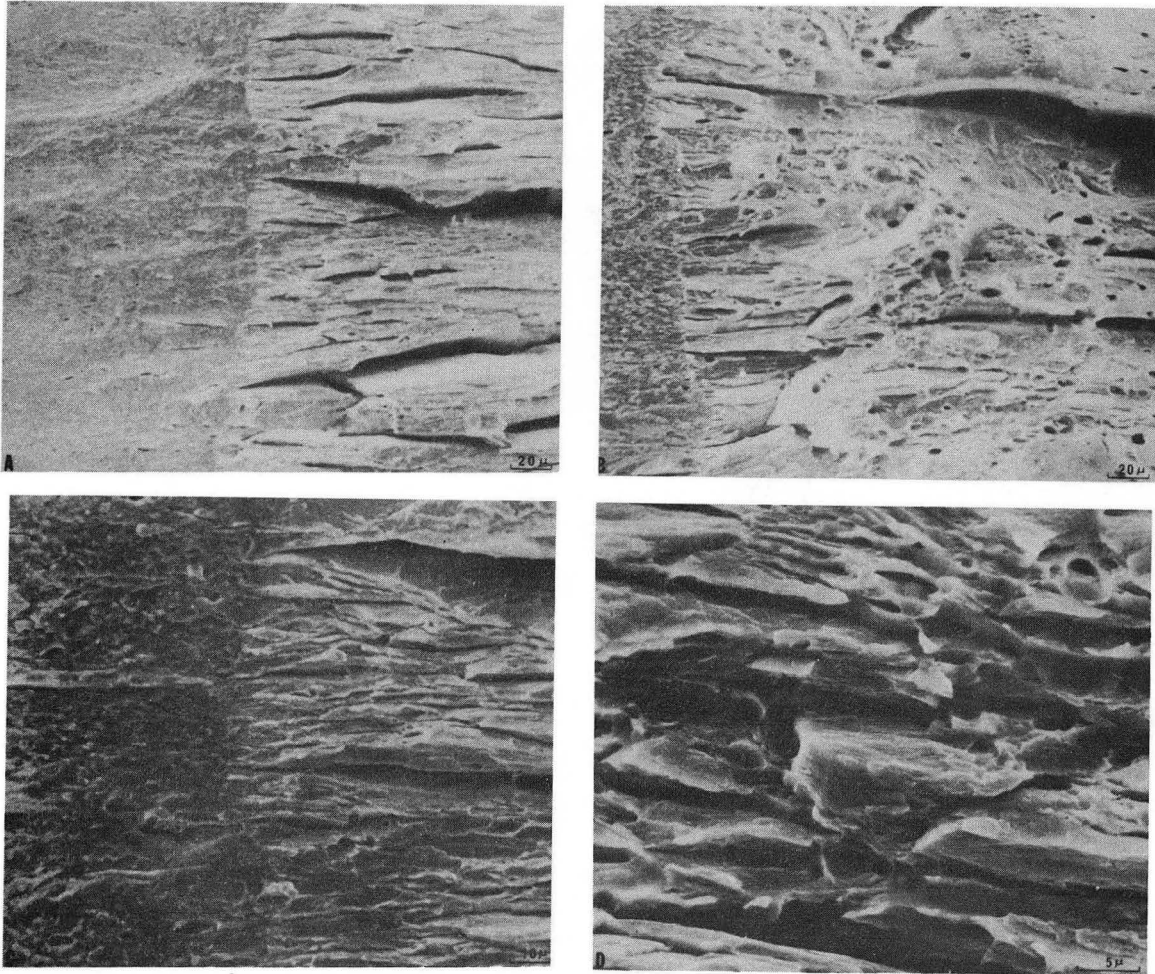Fig. 3 Crack growth rate of TRIP steel SEN specimens tested in 15 psi H_2 as a function of K and T.

XBL719-7265

Fig. 4 Arrhenius plot for slow crack growth of TRIP steel SEN specimens tested in 15 psig H_2.

XBB 719-4366

Fig. 5 SEM fractographs of slow crack growth area of TRIP steel SEN
        specimens held under static load in 15 psig H_2. In (A), (B),
        and (C) fatigue crack region is on the left and slow crack
        growth region is on the right. (D) is slow crack growth area
        at a higher magnification.